Eventually, we obtained 12 monthly 1961-1990 high-resolution direct solar radiation climatologies (based on the *USGS GTOPO30* digital elevation model) and a thirteenth climatology for the average yearly direct solar radiation.

The 1961-1990 direct solar radiation maps for Italy are shown in Chapter 6.5.

### 6.4.2 1961-1990 high-resolution grids for diffuse radiation on real sloped surfaces

#### • Diffuse radiation: assumptions and basic equations

The diffuse solar radiation is the portion of solar radiation that is scattered downwards by the microscopic fluctuations of the molecules in the atmosphere; consequently in a non-interacting atmosphere, the diffuse radiation is null. On clear days, the magnitude of the diffuse radiation is about 10% to 14% of the total solar radiation received by the Earth's surface. On the other hand, on extremely cloudy days, only the diffuse radiation reaches the Earth's surface.

From 1961-1990 monthly high-resolution grids for the diffuse radiation for flat surfaces (calculated as described in Chapter 6.4.6), we calculated 1961-1990 monthly high-resolution grids for the diffuse radiation for sloped surfaces as:

$$H_{dif}^{sloped} = H_{dif}^{flat} \cdot V_F = K_{dif} \cdot H_T^{flat} \qquad \textbf{(190)}$$

Where $V_F$ is the "sky view factor" (see the next paragraph for details), where "sloped" and "flat" are referred to sloped and flat surfaces, and where the last part of the equation can be obtained just by reversing equation (162).

Let us remark that we made two important assumptions: first, we considered the diffuse component of the solar radiation as isotropic as it is usually considered in the majority of solar radiation models (even though it is anisotropic), and second, we considered the diffuse radiation as constant in time during the day, thus it is not necessary to use an integral formula as for the direct radiation.

Eventually, we obtained 12 monthly 1961-1990 high-resolution diffuse solar radiation climatologies (based on the *USGS GTOPO30* digital elevation model) and a thirteenth climatology for the average yearly diffuse solar radiation.

## • Diffuse radiation: the "sky view factor"

A grid cell that is overshadowed does not receive direct radiation, but it may receive diffuse (or rarely reflected) radiation. A surface, whether in shadow or not, can receive diffuse radiation only if the portion of the sky of the overlying atmosphere is unobstructed *(Wang et al., 2006a)*. This introduces the sky view factor, that is the visible fraction of the sky from the grid center *(Wang et al., 2005)*. The so-called sky view factor is usually indicated with $V_F$: if $V_F = 1$, the sky is completely unobstructed, if $V_F = 0$ the sky is totally obstructed and no diffuse radiation reaches the surface *(Antonic, 1998)*. The sky view factor is the multiplying quantity used to convert the diffuse radiation from a horizontal surface to a sloped surface.

The diffuse radiation is the product of the multiple atmospheric scattering. Thus the slope of the grid cell can be considered as the only independent variable for determining the sky view factor, as it can be found in *Chung et al. (2004a), Allen et al. (2006),* and *Coops et al. (2000)*.

The **sky view factor** can be defined as in *Chung et al. (2004a)*:

$$V_F = \frac{1+\cos(s)}{2} = \cos^2\left(\frac{s}{2}\right) \qquad \textbf{(191)}$$

Where, in both equations (191)-(192), $s$ is the slope angle of the sloped surface.

Or, similarly, it can be defined as in *Tian (2001)*:

$$V_F = 0.75 \cdot +0.25 \cdot \cos(s) - \frac{0.5 \cdot s}{\pi} \qquad \textbf{(192)}$$

Where $V_F = 1$ if the surface is flat, $V_F = 0$ if the surface is vertical.

In our models we used the sky view factor as in (191).

### 6.4.3 1961-1990 high-resolution grids for reflected radiation on sloped surfaces

#### • Reflected radiation: assumptions and basic equations

The reflected part of the solar radiation is the solar radiation reflected from a surface.

It depends on three parameters:

- the sum of direct and diffuse radiation ;
- the obstructed portion of the overlying atmosphere;
- the albedo.

Thus, for a sloped surface, we can obtain the reflected solar radiation as:

$$H_{ref}^{sloped} = (H_{dir}^{sloped} + H_{dif}^{sloped}) \cdot O_{SF} \cdot \zeta_g \qquad \textbf{(193)}$$

Where the direct and diffuse component are calculated for the same sloped surface, $O_{SF}$ is the "obstructed sky factor" and $\zeta_g$ is the ground albedo of the surface (see the next paragraphs for details).

Let us make some considerations about the resolution: we used a 1 km$^2$ grid cell, but the reflected radiation is a quantity that should be evaluated at a more local spatial scale. We did not use the average of the sum of diffuse and direct radiation of the 8 grid cells surrounding the grid cell under investigation because a surface does not receive reflected radiation from another surface located 1 km far away. Consequently, we used the obstructed sky factor of the grid cell itself, the direct and diffuse radiation received by the grid cell itself in order to calculate the reflected radiation for the grid cell. We compared results obtained with the two different methodologies all over the Italian area; they differ only by 2% (relative mean absolute error).

Some authors neglect the reflected part of the solar radiation in solar models because it is just a small fraction of the global radiation (it hardly exceeds the 5% of the global radiation, *Coops et al., (2000)*) and it occurs only when a significant portion of the overlying atmosphere is obstructed *(Antonic, 1998)*. The reflected radiation is strictly correlated with

the surrounding topography and it can be received only by a surface that is surrounded by some obstacles. In our opinion, in a wide area with complex orography as Italy and highly reflecting surfaces as the Alpine glaciers, the reflected radiation cannot be neglected.

Eventually, we obtained 12 monthly 1961-1990 high-resolution reflected solar radiation climatologies (based on the *USGS GTOPO30* digital elevation model) and a thirteenth climatology for the average yearly reflected solar radiation.

## • Reflected radiation: the "obstructed sky factor"

The reflected radiation received by a surface depends on the inclination of the surrounding surfaces, but it is common to consider only the inclination of the grid cell under investigation and the "**obstructed sky factor**" that can be defined as the complementary of the sky view factor *(Osozawa et al., 1998; Chung et al., 2004a; Allen et al., 2006)*:

$$O_{SF} = 1 - V_F = 1 - \cos^2\left(\frac{s}{2}\right) \qquad \textbf{(194)}$$

Where $s$ is the slope angle of the sloped surface and $V_F$ is the sky view factor.

Following equation (194), a flat surface does not receive a relevant reflected radiation. This is true with a resolution of 1 km$^2$; with a higher resolution (e.g., 50 m) this can be considered as a rough approximation. Following equation (194), if the surface is flat, the obstructed sky factor is null, thus no reflected radiation is received from the surface; on the other hand, if the surface is vertical, the obstructed sky factor equals 1 and the reflected radiation received from the surface is the highest achievable.

Some authors use a similar quantity, the terrain configuration factor, in order to calculate the reflected radiation. See *Dubayah et al. (1997)*, *Antonic (1998)* or *Wang et al. (2005)* for details.

## • Reflected radiation: the ground albedo

We considered the ground albedo of the grid cell under investigation. We used the *GLC2000* Land Cover high-resolution grid (see Chapter 4) as the land cover grid for Italy. It is divided into 23 sub-categories, but only 15 land cover classes can be found in the Italian territories, as can be seen in the following table.

| GEM class name | In Italy? | Where? |
|---|---|---|
| broad evergreen | No | |
| broad deciduous closed | Yes | Everywhere |
| broad deciduous open | No | |
| needle evergreen | Yes | Alps and High Appennines |
| needle deciduous | No | |
| mixed forest | Yes | Everywhere |
| tree flooded fresh water | No | |
| tree flooded saline water | No | |
| tree/natural vegetation | Yes | < 1% |
| tree burnt | No | |
| shrub evergreen | Yes | Sea coasts (South and Islands) |
| shrub deciduous | Yes | South and Islands (far from the Sea) |
| grass | Yes | Everywhere |
| sparse shrub grass | Yes | Alps |
| flooded shrub grass | No | |
| cultivated managed | Yes | Everywhere but especially in the Po Plain |
| crop/tree/natural vegetation | No | |
| crop/shrub/grass | Yes | Everywhere |
| barren | No | < 1% |
| water | Yes | Sea and Lakes |
| snow ice | Yes | Alpine glaciers |
| artificial surface | Yes | Urban areas |
| irrigated agriculture | Yes | Rice fields in Piedmont |

*Tab. 41: GEM2000 land cover classes distribution in Italy.*

For each of the 15 land cover classes labeled with *"Yes"* in tab. 41, we needed a corresponding albedo value. Recall that the albedo of a surface can be defined as the percentage of the received global radiation that is reflected. If the albedo equals 0.1, it means that only the 10% of the received global radiation will be reflected. The global average albedo is 0.154 *(Henderson-Sellers et al., 1983)*.

In literature we did not find any paper that provides the albedo values for the land cover classes of *GLC2000*, thus we searched for papers or other sources that provide albedo values for the land cover classes from other land cover grids. The reasons why we used the *GLC2000* land cover grid lie in the facts that it provides a detailed description of

methods and data used, it is the only one that shows no remarkable errors, for example in coastlines, and it has the same resolution and coordinates as *USGS GTOPO30 DEM*.

The vast majority of the papers provided albedo values as:

- separated black sky (the reflectance of a surface under direct illumination with no diffuse component), or white sky (the reflectance of a surface under diffuse illumination with no direct component) albedo values as *Csiszar et al. (1999), Strugnell et al. (2001), Zhou et al. (2003), Jin et al. (2004), Moody et al. (2005), Gao et al.(2005) and Barlage et al. (2005,* from *MODIS* (MODerate Resolution Imaging Spectrometer, *http://modis.gsfc.nasa.gov/*) or *AVHRR* (Advanced Very High Resolution Radiometer, *http://noaasis.noaa.gov/NOAASIS/ml/avhrr. html*) ;
- single land cover class albedo values, e.g. are: for urban areas by *Oke (1982)*, *Taha (1997),* for one or more forest categories by *Stanhill et al. (1966), Betts et al. (1997), Lyons et al. (2008)*, for crop categories by *Barker et al. (1989), Jacobs et al. (1990), Betts et al. (1997), Schaaf et al. (2002), Betts et al. (2007),* types of desert sand by *Ten Berge (1986)*, shrubs by *Domingo et al. (2000)*, oceans by *Hummel et al. (1979)* or other categories by *Campbell et al. (1998), Dorman et al. (1989), Scharmer et al. (2000), Masson et al. (2003), Champeaux et al. (2004)* ;
- albedo values obtained with measurements at a too local scale for our purposes as in *Stewart (1971), Laine et al. (1996), Christen et al. (2004)* ;
- albedo values referred only to a single month or to a single season as in *Briegleb et al. (1986), Strugnell et al. (2001), Wei et al. (2001), Zhou et al. (2003), Jin et al. (2004).*

On the other hand, we needed monthly (or seasonal) broadband albedo values and we found four papers that provided us with globally valid albedo values:

- *Wilson et al. (1985)*: summer, winter, yearly average albedo values for 26 land cover classes ;
- *Hummel et al. (1979) and Henderson-Sellers et al. (1983)*: spring, summer, fall, winter albedo values (snow-covered and snow-free surfaces) for 13 land cover classes ;
- *Matthews (1984)*: spring, summer, fall, winter albedo values (snow-free surfaces) for 32 land cover classes.

For our solar radiation models we calculated the average, for each category, of the albedo values of the last four papers listed above and we used albedo values from local studies where necessary.

We made some assumptions: we did not consider the snow cover in winter, but for the permanent snow/ice land cover class, even though from November to March in the Alpine region and in some large Northern areas of Italy, the surfaces may be covered by snow. In the future, we plan to study a model that takes the seasonal snow cover into account.

Next, we applied the seasonal albedo values to our monthly calculations: spring is referred to March, April and May, summer to June, July and August, fall to September, October and November, winter to December, January and February.

In the following table we show the albedo values used to calculate the monthly high-resolution grids for reflected radiation (and global and absorbed radiation, see next paragraphs). Let us notice that for "mixed forest", we used the mean value between deciduous and evergreen forest; for all the other categories we found corresponding albedo values in literature.

| *GEM* class name | winter | spring | summer | fall |
|---|---|---|---|---|
| *broad deciduous closed* | *0.14* | *0.14* | *0.15* | *0.15* |
| *needle evergreen* | *0.11* | *0.13* | *0.11* | *0.13* |
| *mixed forest* | *0.13* | *0.14* | *0.13* | *0.14* |
| *tree/natural vegetation* | *0.15* | *0.15* | *0.13* | *0.14* |
| *shrub evergreen* | *0.17* | *0.15* | *0.17* | *0.17* |
| *shrub deciduous* | *0.19* | *0.17* | *0.19* | *0.19* |
| *grass* | *0.19* | *0.19* | *0.19* | *0.19* |
| *sparse shrub grass* | *0.18* | *0.18* | *0.21* | *0.19* |
| *cultivated managed* | *0.15* | *0.16* | *0.19* | *0.16* |
| *crop/shrub/grass* | *0.18* | *0.18* | *0.19* | *0.19* |
| *barren* | *0.17* | *0.21* | *0.30* | *0.23* |
| *water* | *0.07* | *0.07* | *0.07* | *0.07* |
| *snow ice* | *0.75* | *0.68* | *0.68* | *0.68* |
| *artificial surface* | *0.16* | *0.16* | *0.16* | *0.16* |
| *irrigated agriculture* | *0.12* | *0.12* | *0.12* | *0.12* |

*Tab. 42: albedo values used in solar radiation models for Italy*

It can be easily seen that the reflected radiation is usually a small fraction of the total incoming radiation: e.g., if the albedo is 0.15 (spring, shrub evergreen) and the obstructed sky factor is 0.2, the reflected component is just the 3% out of the global radiation.

Reflected radiation ranges from 0% out of the global radiation (flat surface) to 75% out of the global radiation (winter, vertical surface, snow or ice). Over real surfaces it hardly exceeds 5% and in the majority of the Italian grid cells it is smaller than 1%.

These albedo values were also used to calculated high-resolution monthly global radiation and absorbed radiation grids as we discuss in the next paragraphs.

### 6.4.4 1961-1990 high-resolution grids for global radiation on sloped surfaces

The global radiation received by a sloped surface can be obtained as the sum of three components, direct radiation, diffuse radiation and reflected components, as:

$$H_{GLOBAL}^{sloped} = (H_{dir}^{sloped} + H_{dif}^{sloped} + H_{refl}^{sloped}) \cdot \quad \textbf{(195)}$$

We obtained 12 monthly 1961-1990 high-resolution global solar radiation climatologies (based on the *USGS GTOPO30* digital elevation model) and a thirteenth climatology for the average yearly global solar radiation. Such grids were used in the temperature climatologies described in Chapter 4.

The 1961-1990 direct solar radiation maps for Italy are shown in Chapter 6.6. Whilst diffuse and reflected solar radiation maps are not shown in this thesis, but data grids and maps are available upon request.

### 6.4.5 1961-1990 high-resolution grids for absorbed radiation on sloped surfaces

The solar radiation absorbed by a surface can be an important quantity for, e.g., energy applications. It can be calculated as:

$$H_{Absorbed}^{sloped} = (1 - \varsigma_g) \cdot H_{GLOBAL}^{sloped} \quad \textbf{(196)}$$

Where $\zeta_g$ is the ground albedo. The absorbed radiation is the global radiation received and not reflected away by the surface.

We obtained 12 monthly 1961-1990 high-resolution absorbed solar radiation climatologies (based on the *USGS GTOPO30* digital elevation model) and a thirteenth climatology for the average yearly absorbed solar radiation.

The monthly 1961-1990 absorbed solar radiation maps for Italy are shown in Chapter 6.6.

## 6.5 Validation

The solar radiation models are rarely validated because they are not based on real data, but rely on astronomical parameters, on calculations on topographic quantities and on a-priori approximations only and provide exact results even though in some cases such results are unrealistic (e.g., the clear sky models).

Our solar model is based on sunshine duration records and provides solar radiation grids, thus we cannot use sunshine duration data in order to validate the model. On the other hand, we used the small set (33 records) of 1961-1990 global radiation stations found in the Italian Air Force (Aeronautica Militare Italiana) website and evaluated the mean absolute error and the relative mean absolute error as for temperature and precipitation models. The small number of records did not allow us to perform a cross validation or a jack-knife validation.

We also found no data to validate the direct, the diffuse, the reflected or the absorbed radiation grids.

In the next page, in table 43, we show the table of the statistical parameters used for validation, i.e. the monthly *MAE* in MJ/m² and the relative *MAE*, the so called *MAER*, in percentage (%).

| | MAE ($MJ/m^2$) | MAER (%) |
|---|---|---|
| Jan | 0.27 | 4.4 |
| Feb | 0.31 | 3.5 |
| Mar | 0.45 | 3.4 |
| Apr | 0.86 | 4.9 |
| May | 0.78 | 3.6 |
| Jun | 1.05 | 4.4 |
| Jul | 1.16 | 4.8 |
| Aug | 0.97 | 4.6 |
| Sep | 0.81 | 5.0 |
| Oct | 0.55 | 5.1 |
| Nov | 0.36 | 5.3 |
| Dec | 0.33 | 6.3 |
| Year AVG | **0.66** | **4.6** |

*Tab. 43: Monthly MAE (in $MJ/m^2$) and MAER in % for global solar radiation grids*

As expected, the *MAE* is smaller in winter than in summer because global radiation in winter is smaller. The average *MAER* is under the threshold of 5%.

It should be underlined that we compared the global radiation data of the Air Force records with the global radiation data modelled for the corresponding grid cell. This could lead to an overestimation of the statistical errors because a grid cell has a slope value and an aspect value that, in areas with a complex orography, hardly correspond to the slope and aspect values of the surface where the station is located. An average relative mean absolute error smaller than 5% can be considered a very good result.

Let us show, in the next page, a comparison between real data from the Air Force dataset and the modelled global solar radiation data of our 1961-1990 high-resolution climatologies for Italy. It can be seen that our model provides better estimations for stations located in plains and on the sea's coast than for stations located in areas with complex orography, as expected.

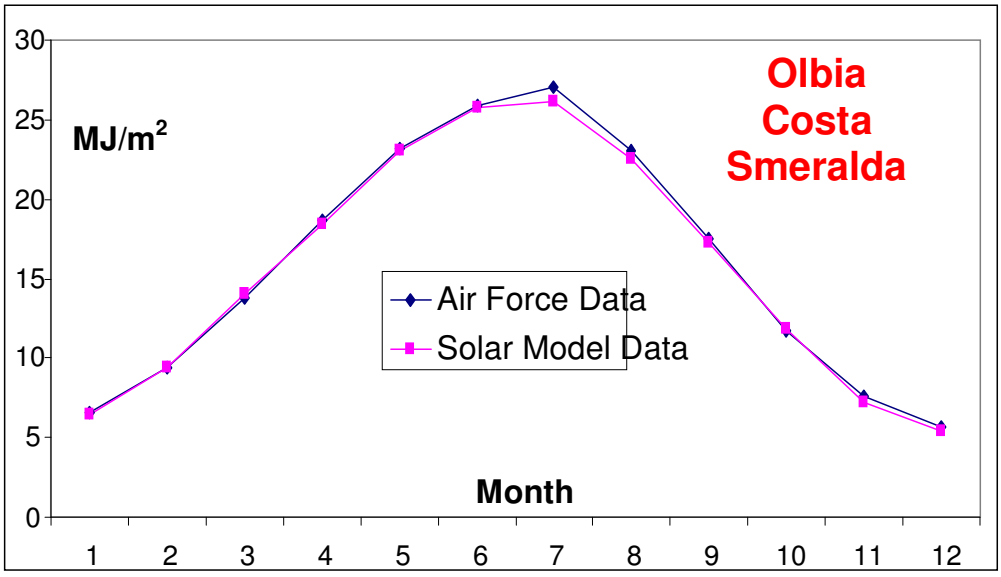


*Fig. 176: Comparison between measured data and modeled data for Olbia station.*

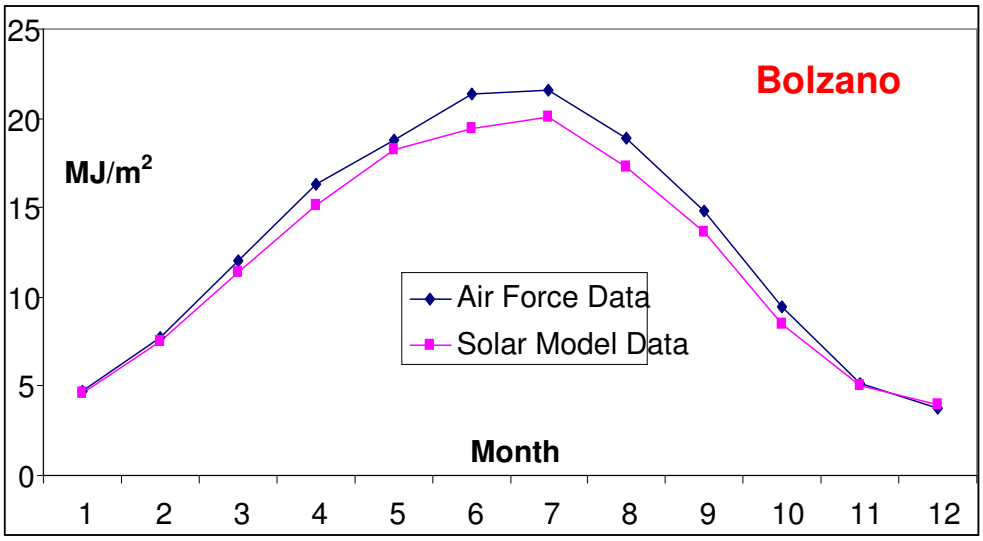


*Fig. 177: Comparison between measured data and modeled data for Bolzano station.*

## 6.6 High-resolution 1961-1990 solar radiation maps for Italy

In the next pages we show the monthly 1961-1990 climatologies for the direct radiation, global radiation and absorbed radiation for sloped surfaces (as in *USGS GTOPO30* digital elevation model).

The 12 monthly maps and the yearly map (obtained as the average of the 12 monthly radiation values) are expressed in Mj/m² and the values represent the daily total for the "mean day" of each month. In every map, the radiation scale ranges from 0 (it happens for narrow valleys in winter for direct radiation) to 30 Mj/m² (maximum value in the map is approximately 28 Mj/m² on the south-facing slope near the top of Volcano Etna in June for global radiation). In the maps, the white areas within Italy correspond to grid cells labeled with "water" in the *GEM2000* land cover grid, including lakes and rivers, where we did not calculate solar radiation values.

## • Direct solar radiation

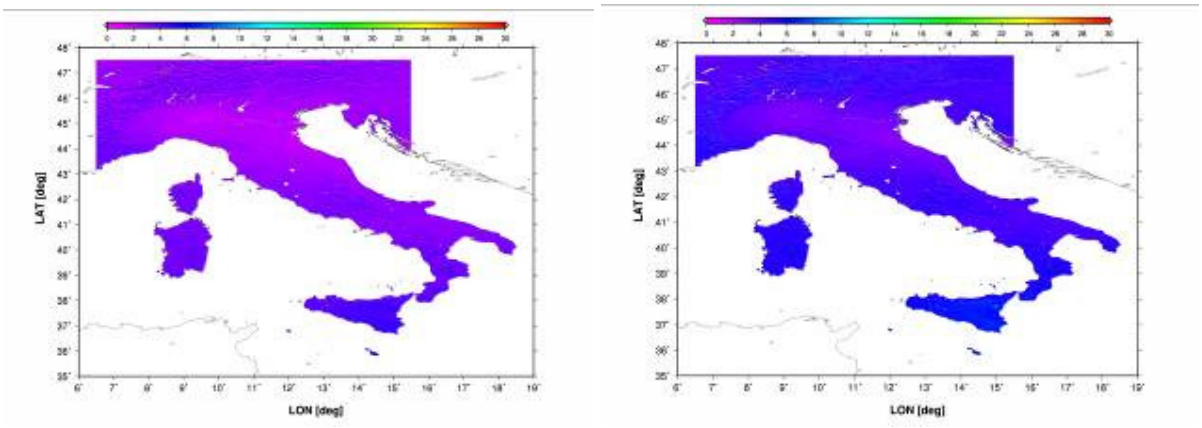


*Fig. 178-179: 1961-90 January and February direct solar radiation maps*

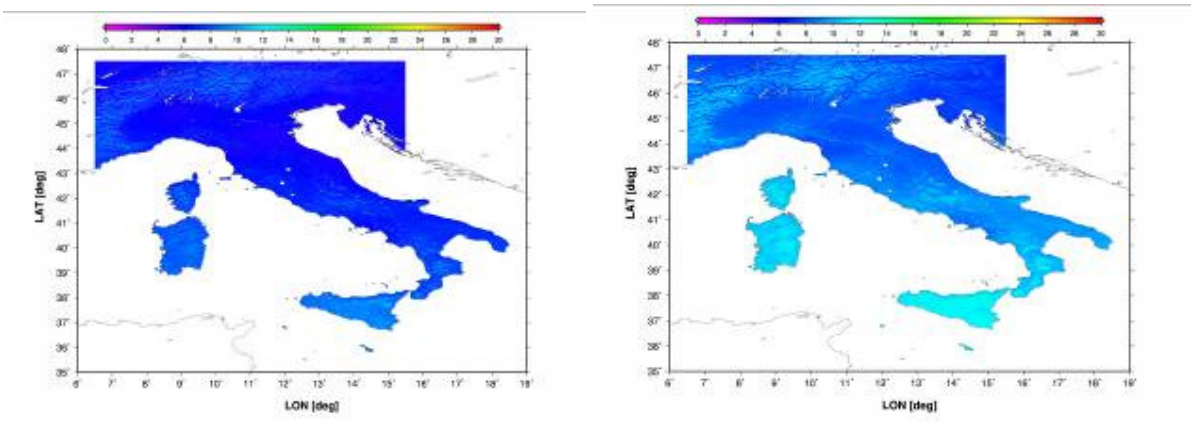


*Fig. 180-181: 1961-90 March and April direct solar radiation maps*

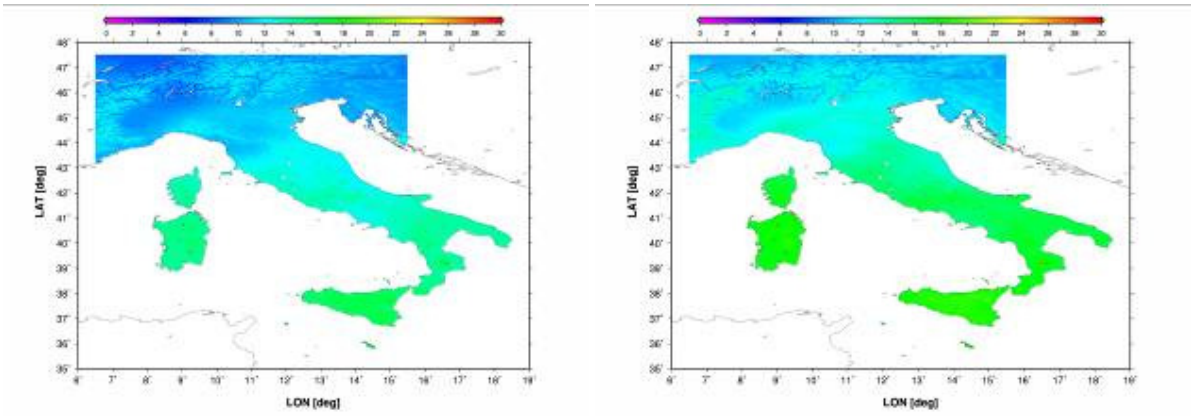


*Fig. 182-183: 1961-90 May and June direct solar radiation maps*

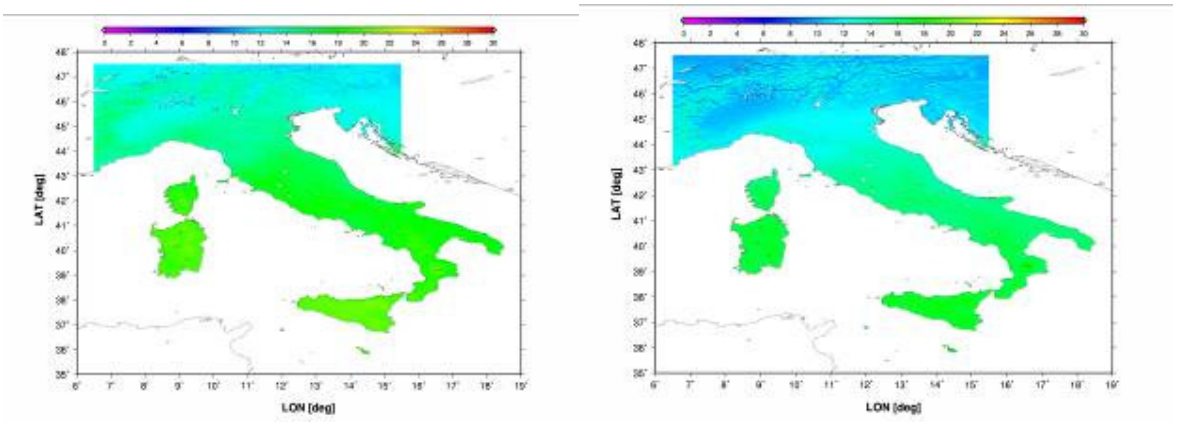


*Fig. 184-185: 1961-90 July and August direct solar radiation maps*

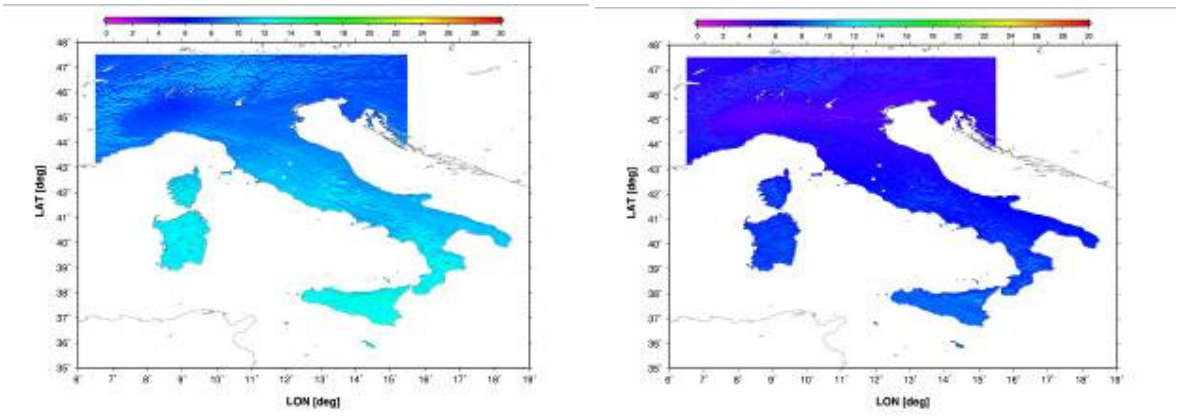


*Fig. 186-187: 1961-90 September and October direct solar radiation maps*

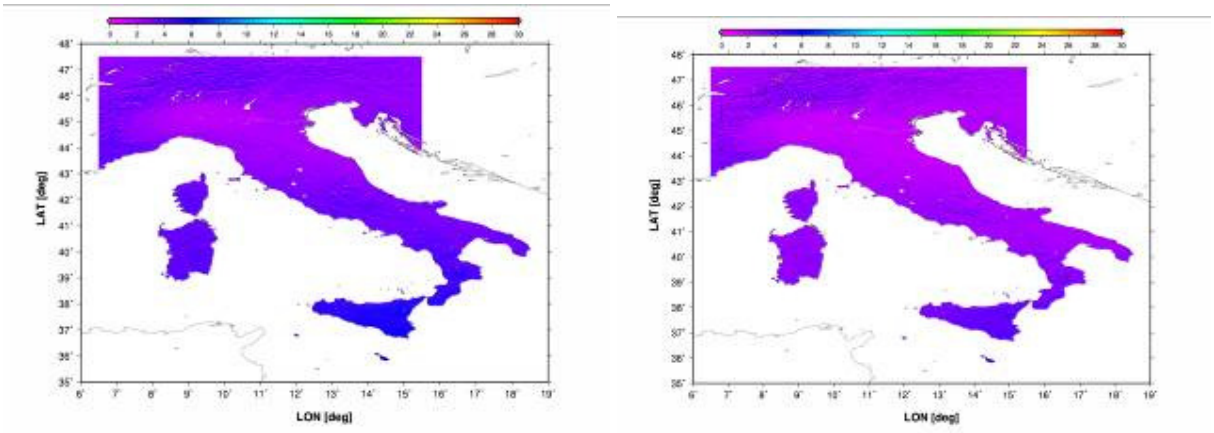


*Fig. 188-189: 1961-90 November and December direct solar radiation maps*

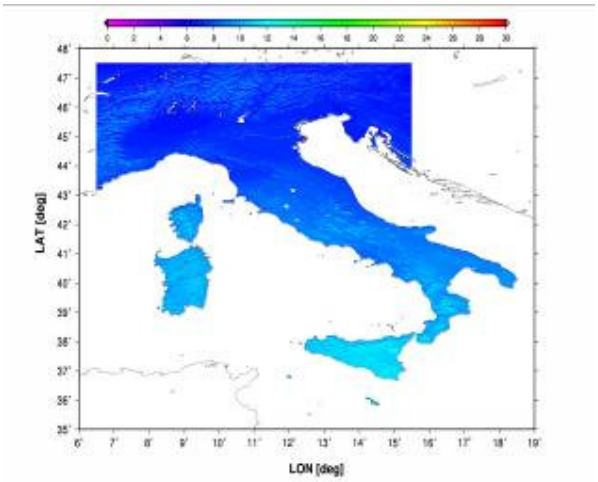


*Fig. 190: 1961-90 Average Yearly direct solar radiation maps*

## • Global solar radiation

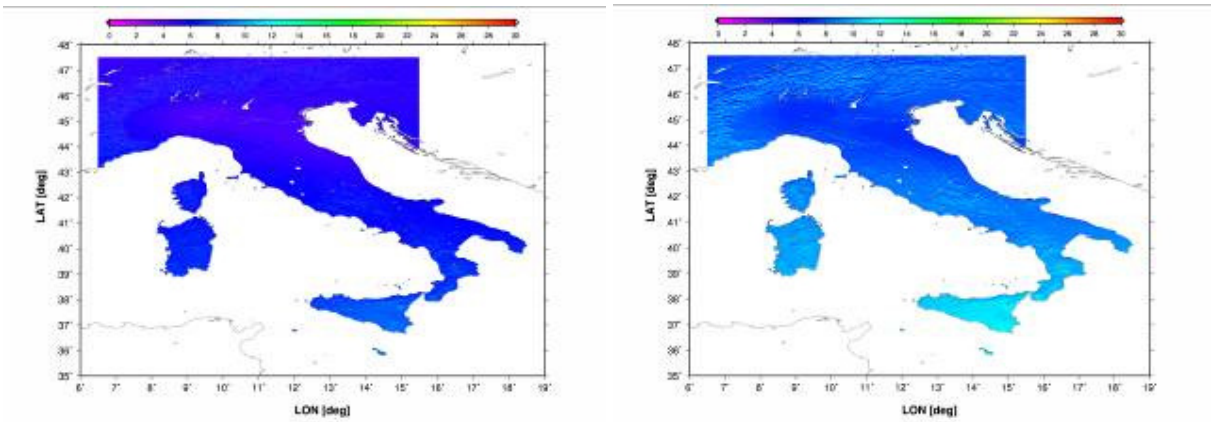


*Fig. 191-192: 1961-90 January and February global solar radiation maps*

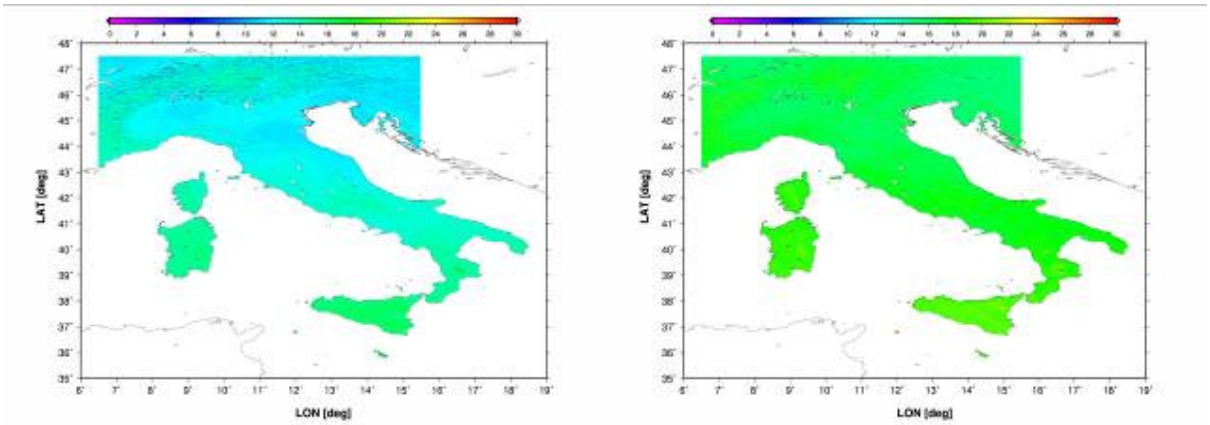


*Fig. 193-194: 1961-90 March and April global solar radiation maps*

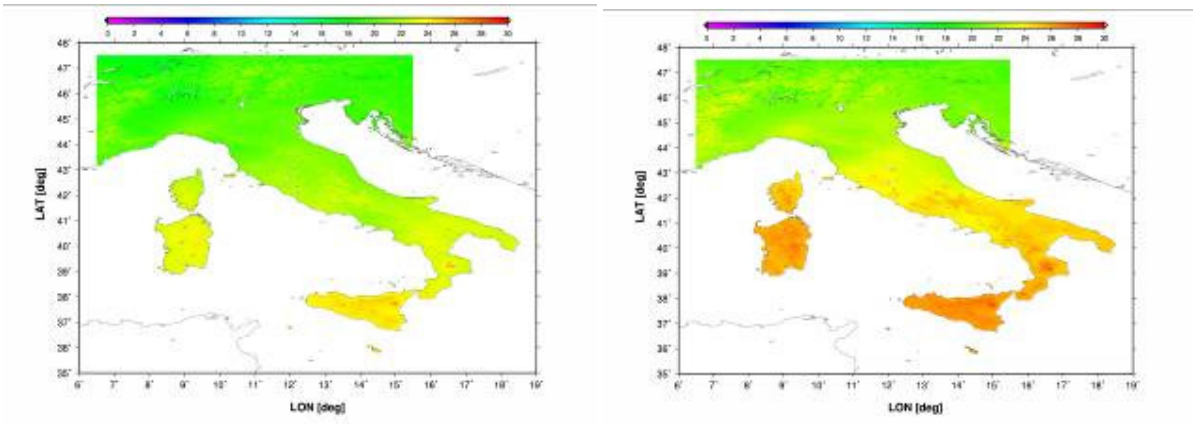


*Fig. 195196: 1961-90 May and June global solar radiation maps*

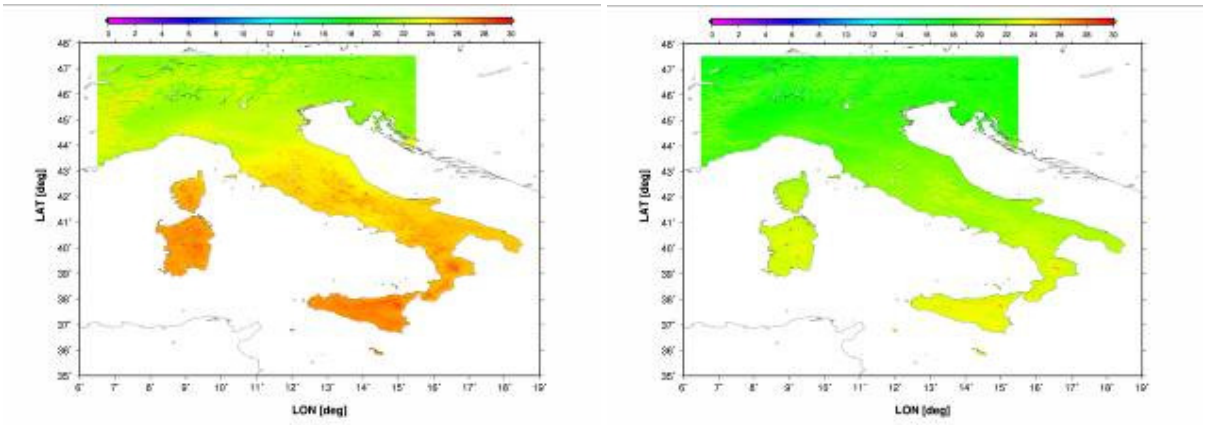


*Fig. 197-198: 1961-90 July and August global solar radiation maps*

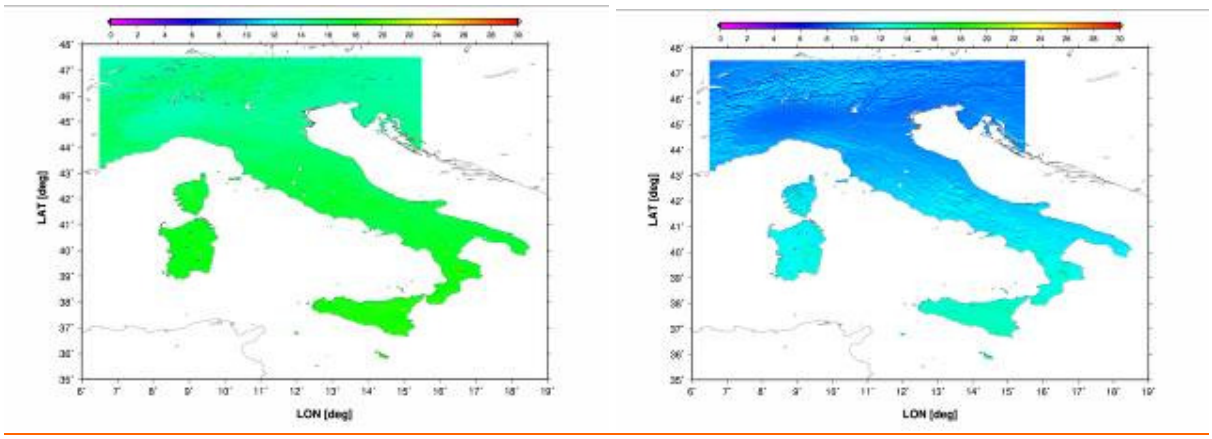


*Fig. 199-200: 1961-90 September and October global solar radiation maps*

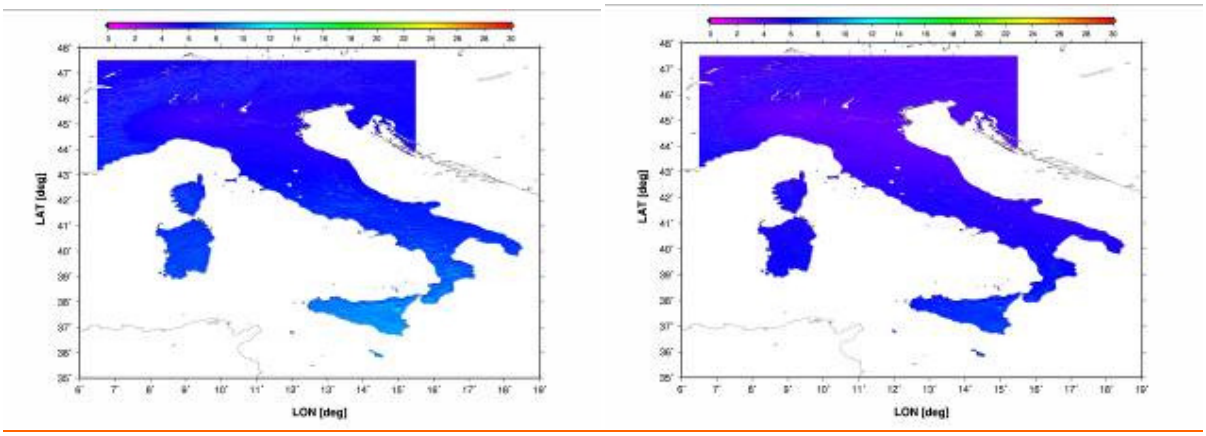


*Fig. 201-202: 1961-90 November and December global solar radiation maps*

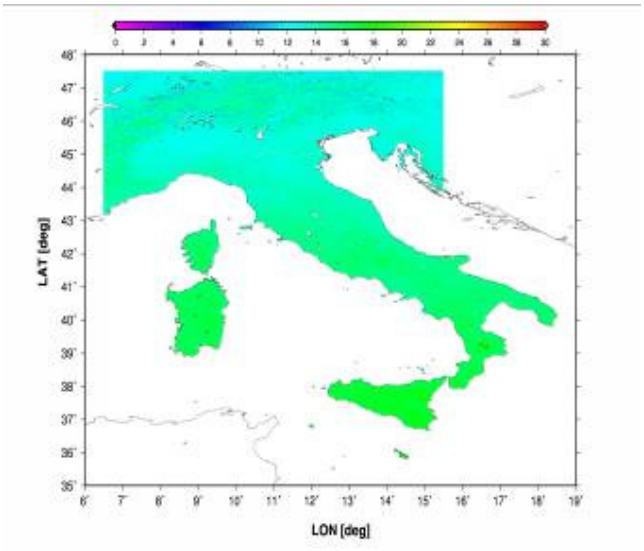


*Fig. 203: 1961-90 Average Yearly global solar radiation maps*

- **Absorbed solar radiation**

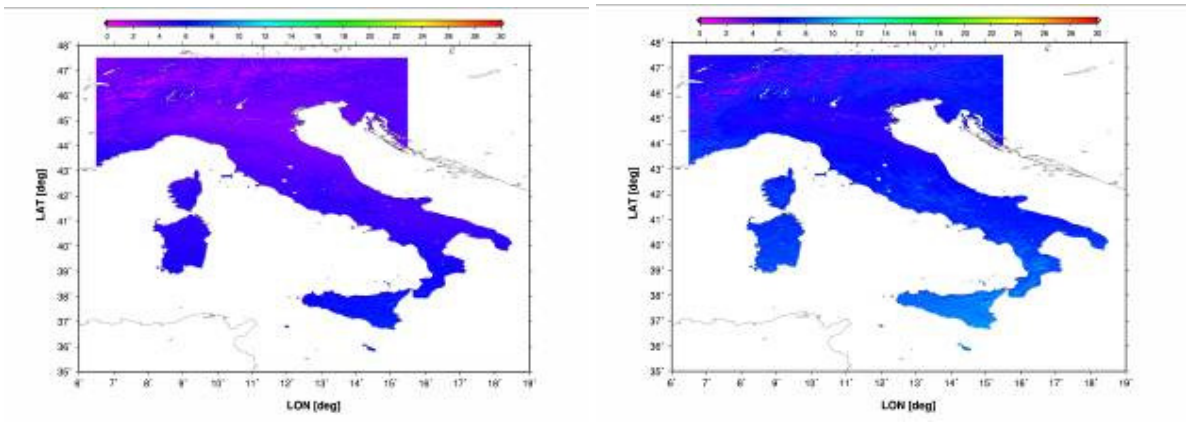


*Fig. 204-205: 1961-90 January and February absorbed solar radiation maps*

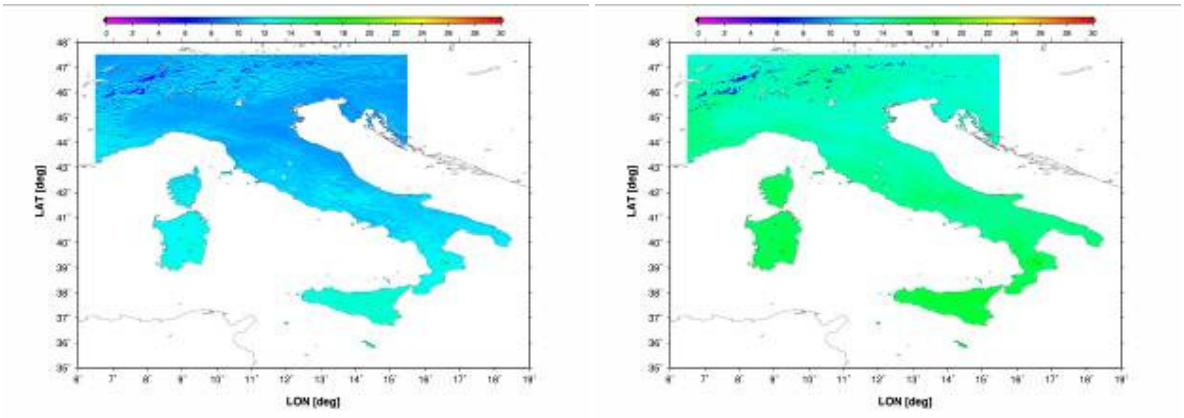


*Fig. 206-207 1961-90 March and April absorbed solar radiation maps*

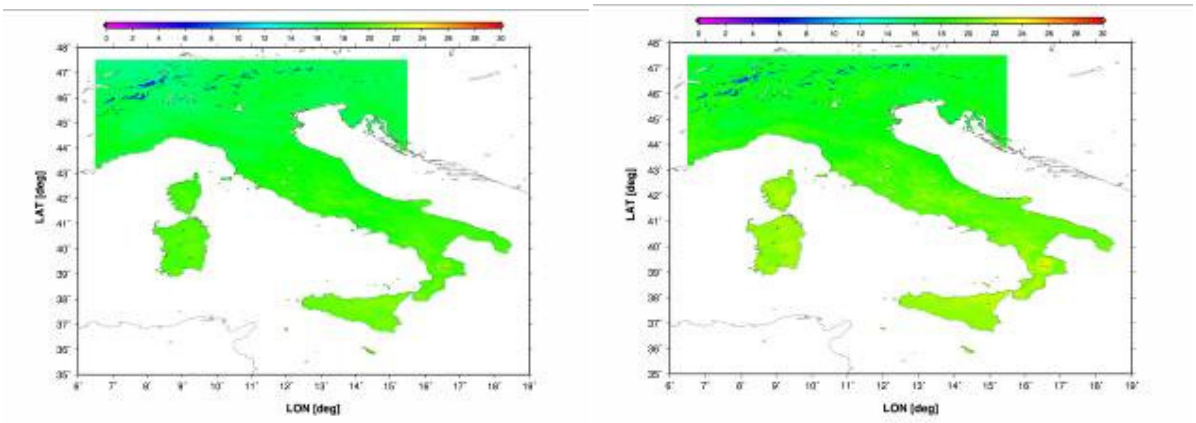


*Fig. 208-209: 1961-90 May and June absorbed solar radiation maps*

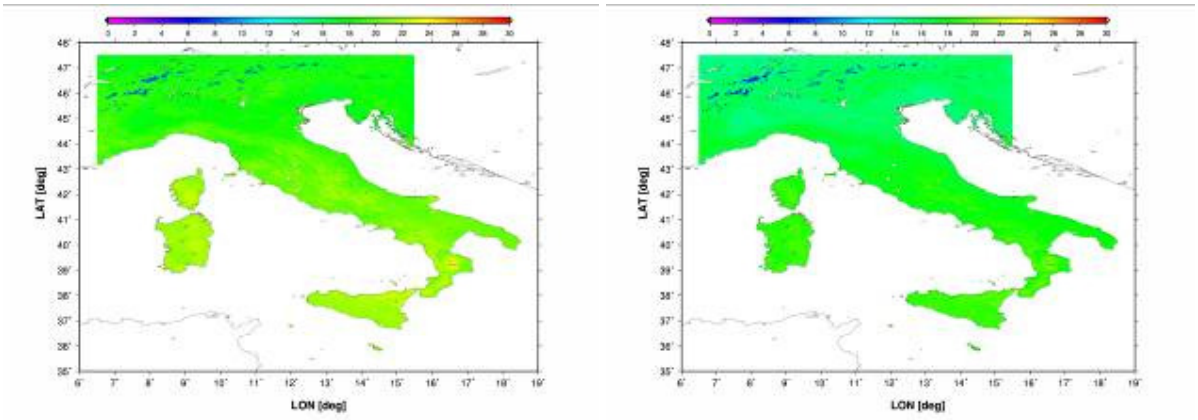


*Fig. 210-211: 1961-90 July and August absorbed solar radiation maps*

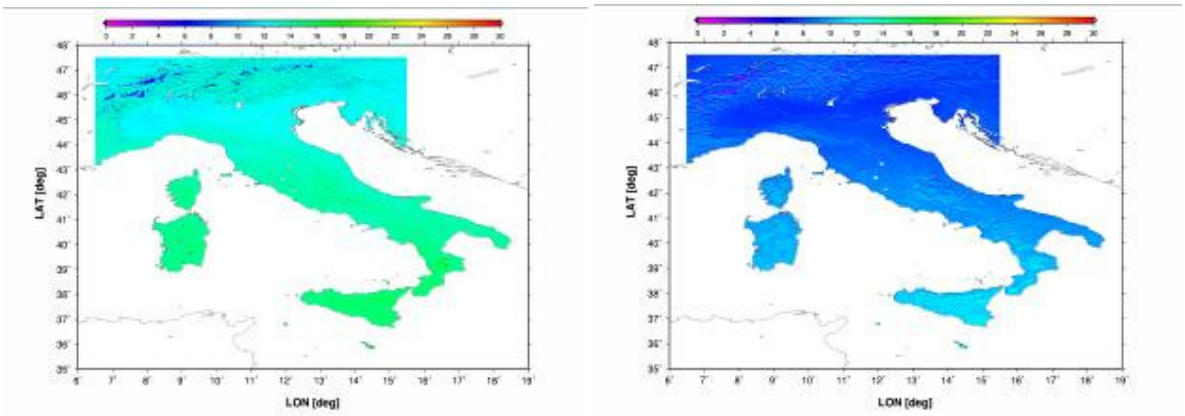


*Fig. 212-213: 1961-90 September and October absorbed solar radiation maps*

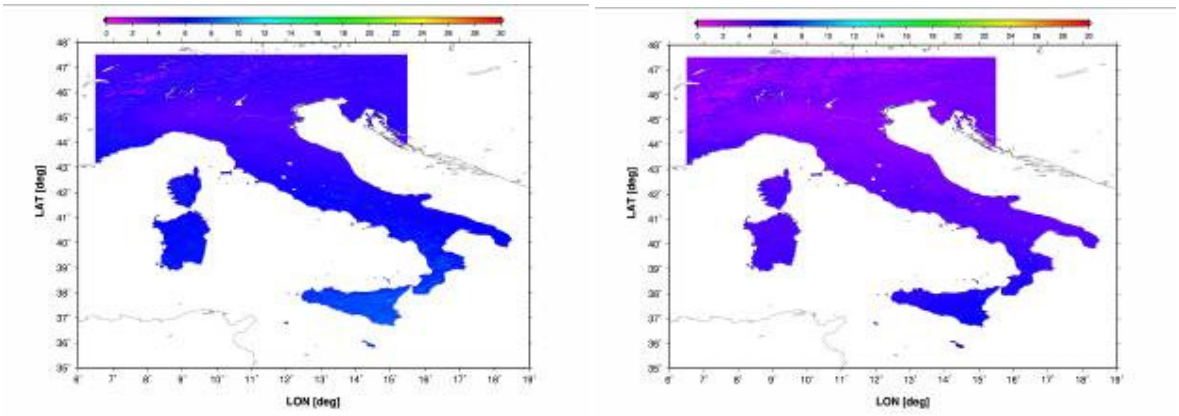


*Fig. 214-215: 1961-90 November and December absorbed solar radiation maps*

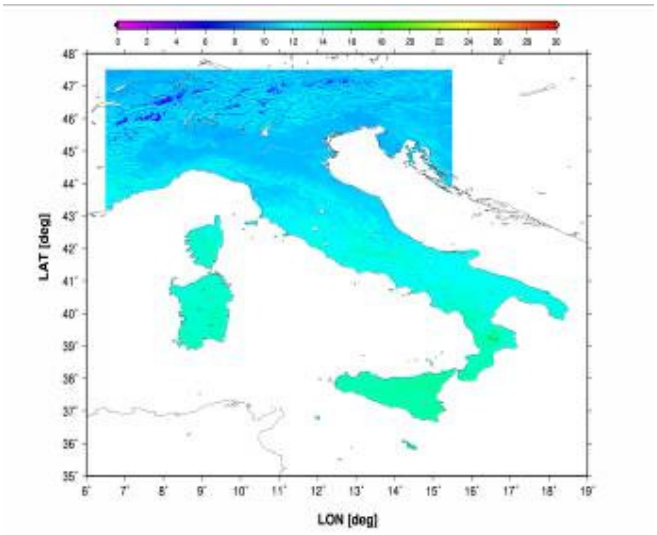


*Fig. 216: 1961-90 Average Yearly absorbed solar radiation maps*